Bull. Mater. Sci., Vol. 38, No. 5, September 2015, pp. 1315–1327. © Indian Academy of Sciences.

Non-isothermal crystallization kinetics and thermal behaviour of PA12/SEBS-*g*-MA blends

KHUSHBOO RINAWA[1], S N MAITI[1,*], R SONNIER[2] and J-M LOPEZ CUESTA[2]

[1]Centre for Polymer Science and Engineering, Indian Institute of Technology Delhi, Hauz Khas, New Delhi 110 016, India

[2]Centre des Matériaux de Grande Diffusion, Ecole des Mines d'Alès, 6, Avenue de Clavières, 30318 Alès Cedex, France

MS received 2 March 2015; accepted 18 May 2015

Abstract. The thermal behaviour and crystallization kinetics of PA12/SEBS-*g*-MA blends were investigated under non-isothermal and isothermal conditions using thermogravimetric analysis and differential scanning calorimetry, respectively. The macrokinetic model given by Avrami was used to analyse both the non-isothermal and isothermal crystallization kinetics of the blends. The value of the Avrami exponent during non-isothermal crystallization predicted that pure PA12 and PA12/SEBS-*g*-MA blends show spherulitic growth with random nucleation of crystal structures as the *n*-values lie between 3 and 4. The slight nucleating effect of SEBS-*g*-MA was showed by nucleating activity calculated by the Dobreva and Gutzowa method.

Keywords. Crystallization kinetics; Avrami; PA12; DSC; activation energy.

1. Introduction

Thermal stability and crystallization behaviour of polymer blends have been of great concern in recent years, as they provide fruitful information about the behaviour of blends. Crystallization of semi-crystalline polymers is a combined process of nucleation and growth of crystals from the molten state.[1,2] Therefore, it is controlled by both the rate of transformation/nucleation and the rate of crystal growth. The macrokinetic model proposed by Avrami is generally used to describe the kinetics of crystallization, i.e., transformation of one phase to another under isothermal conditions. Generally, isothermal crystallization conditions are rarely used in practice because all the industrial processes such as extrusion, injection molding, film blowing, foaming proceed in continuously changing thermal environment, i.e., under non-isothermal condition.[3,4] It has been reported that the crystalline behaviour of polymer blend is greatly influenced by the size, shape, dispersion of dispersed particles and phase adhesion between the components of blend.

The valuable combination of typical nylon and polyolefin properties has increased the use of long aliphatic chain polyamides (PA) in military, machinery, multiple engineering applications particularly in automotive and electrical industries.[5–7] A major limitation of PA is its inherently low impact strength, especially at low temperature. Hence, blending of PA with elastomers has been extensively used to make them suitable for versatile engineering applications. The thermal property and crystallization behaviour of these blends greatly influence the polymer properties through the crystal structure and morphology generated. Hence, it is desirable to study the thermal behaviour and crystallization kinetics of PA/elastomer blends in both the isothermal and non-isothermal conditions. Several reports have described the kinetic of crystallization using different kinetic models.[2]

The aim of the study is to observe the thermal behaviour of PA and SEBS-*g*-MA blend. This is important in analysing the processing conditions during injection molding while one want to fabricate an article of these blends, as the crystallization behaviour has important impact on the final behaviour of blends.

In the present study, polyamide 12 (PA12) has been impact modified by blending it with SEBS-*g*-MA copolymer. The morphology and crystallization behaviour of the blend depends on the nucleating activity of the copolymer added and the phase separation between the two polymers. Depending upon the blend compositions, SEBS-*g*-MA can show drastic change in the overall crystallization behaviour of PA12. Activation energy of crystallization was evaluated to get information on the thermal stability of blend and change in crystallization behaviour of PA12 with the addition of 0–50 wt% of SEBS-*g*-MA copolymer.

*Author for correspondence (maitisn49@yahoo.co.in)

2. Experimental

2.1 *Materials*

PA12 (Vestamid L 2140) used was a commercial product from Evonik Degussa High Performance Polymers, Germany. The melt-volume-flow rate (275°C, 5 kg load) and density of PA12 were 36 cm^3/10 min and 1.01 g cm^{-3}, respectively. SEBS-*g*-MA with 1.4–2.0 wt% MA graft ratio and MFI of 22 g/10 min (230°C, 5 kg load) were obtained from Kraton Polymers. SEBS-*g*-MA (specific gravity of 0.91 g cm^{-3}) contained a styrene/rubber ratio 30/70%, while the average-number molecular weights (M_n) of the PS and poly(ethylene-*co*-butylene) copolymer were of approximately 7000 and 37,500 g mol^{-1}, respectively.[8]

2.2 *Sample preparation*

PA12 and SEBS-*g*-MA pellets were dehumidified in a vacuum oven at 80°C for 18 and 12 h, respectively. Melt mixing of the components was carried out on a co-rotating twin-screw extruder, Clextral, 900 mm (L/D = 42) at a screw speed of 300 rpm. The extrusion zone temperature ranged from 220 to 240°C. Thick strands leaving the extruder die were water cooled, dried and chopped into granules which were subsequently dried in vacuum at 80°C for 12 h. The blends were injection-molded on a Krauss Maffei (CX series) injection-molding machine, into standard tensile bars with 4 mm thickness according to ISO 3167 test procedure. The melt and mold temperatures were maintained at 220–240 and 40°C, respectively. The blends were designated as NS5, NS10, NS20, NS35 and NS50 containing 5, 10, 20, 35 and 50 wt% of SEBS-*g*-MA co-polymer (table 1).

2.3 *Measurements*

2.3a *Thermogravimetric analysis (TGA):* The relative thermal stability of various blends in nitrogen atmosphere was determined using Perkin Elmer Pyris 1 TGA. The investigations were performed in the temperature range of 50–750°C. The relative thermal stability of the extruded samples was evaluated by comparing the onset decomposition temperature (5 and 10 wt% loss temperature), peak decomposition temperature (T_{peak}) and peak decomposition rate.

2.3b *Differential scanning calorimetry (DSC):* DSC measurements were carried out on a Perkin Elmer Pyris Diamond differential scanning calorimeter. The samples obtained by scraping small chips from the injection-molded samples were dried in a vacuum oven at 80°C for 12 h before starting the experiment. About 4–6 mg of the polymer samples was weighed accurately in the aluminium pan and placed in the DSC cell. For the non-isothermal crystallization studies, the samples were heated at a constant heating rate (10, 20 and 30°C min^{-1}) from room temperature to 250°C and held there for 2 min to eliminate the residual crystals and memory effects due to thermal history, and then cooled to crystallize at the same cooling rate under nitrogen environment to room temperature.

For isothermal crystallization kinetics, the samples were heated at a constant heating rate of 30°C min^{-1} from room temperature to 250°C and held there for 2 min to eliminate the thermal history, then the melt was cooled at the same rate upto 148°C and kept constant at 148°C for 10 min until the sample completely crystallized.

3. Results and discussion

3.1 *TGA*

The onset decomposition temperature (T_{onset}), temperature at 5 wt% loss, peak decomposition temperature (T_{peak}), end temperature (T_{end}) and peak decomposition rate of respective blend compositions are given in table 2. Neat PA12 and the blends show single-step decomposition in the nitrogen atmosphere. The end degradation temperatures were almost same for all the compositions. There was not much change in the peak decomposition temperature of PA12 by adding 5–20 wt% of SEBS-*g*-MA but with further increase in SEBS-*g*-MA content, the parameter reduces by 4–9°C. This may be due to the enhanced SEBS-*g*-MA concentration as the T_{peak} of the latter is very less.

Table 1. Blend compositions.

Sample designation	PA12 (wt%)	SEBS-*g*-MA (wt%)	Φ_d
N12	100	0	0.00
NS5	95	5	0.05
NS10	90	10	0.11
NS20	80	20	0.21
NS35	65	35	0.37
NS50	50	50	0.52

Table 2. TGA data for PA12, SEBS-*g*-MA and their blends.

Sample	T_{onset} (°C)	T_{peak} (°C)	T_{end} (°C)	Peak decomposition rate (% min^{-1})
N12	431.5	473.1	495.4	23.7
NS5	432.6	471.7	494.1	24.4
NS10	441.2	473.6	494.4	26.2
NS20	441.1	474.4	491.9	26.7
NS35	440.0	469.7	492.5	26.8
NS50	426.1	464.4	499.6	21.4
SEBS-*g*-MA	416.0	456.5	486.7	22.1

However, the addition of 10–35 wt% of rubber into PA12 matrix improves the onset degradation temperature by about 10°C. This increase can be attributed to chemical interaction between PA12 and grafted maleic group of SEBS, which could have decomposed at further increase in temperature resulting in a decrease in peak decomposition temperature and faster decomposition.

3.2 *Non-isothermal crystallization kinetics*

The crystallization exotherms of PA12 and PA12/SEBS-*g*-MA blends with 10, 20, 35 and 50 wt% of SEBS-*g*-MA recorded at cooling rates of 10, 20 and 30°C min^{-1} are shown in figure 1a–e. All the samples show distinct single exothermic peak at different cooling rates in the temperature range of 130–160°C. It is evident from these curves that with increasing cooling rate the crystallization exotherms become wider and shift towards lower temperature range. The onset crystallization temperature (T_0), peak crystallization temperature (T_p) and undercooling temperature ($\Delta T_c = T_m - T_p$, T_m is the endothermic peak melting temperature) are listed in table 3. Both T_0 and T_p shift to slightly lower temperature with increase in cooling rate (R). This is due to the fact that higher

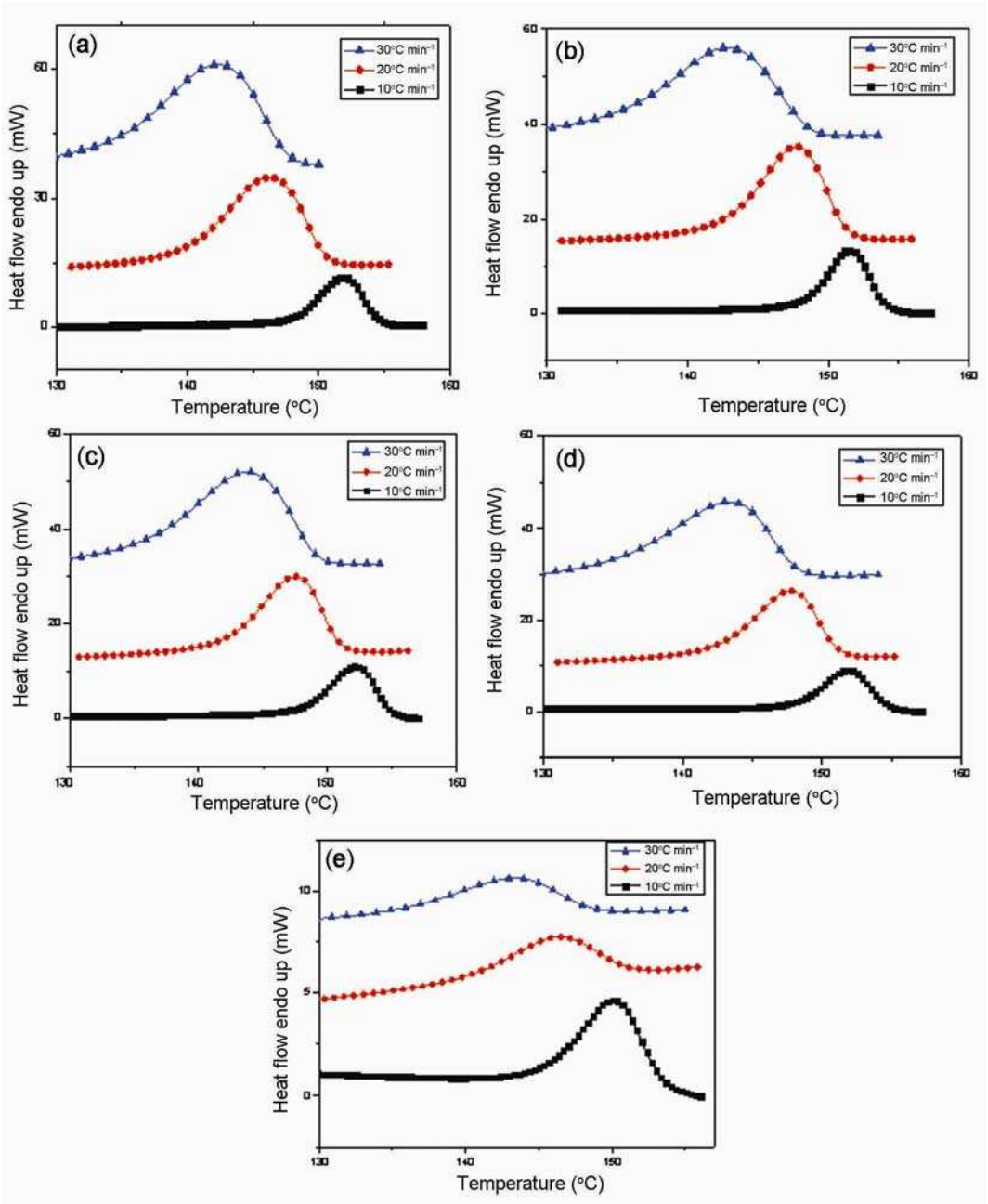

Figure 1. DSC cooling scans of PA12/SEBS-*g*-MA blends at various cooling rates: (**a**) N12, (**b**) NS10, (**c**) NS20, (**d**) NS35 and (**e**) NS50.

Table 3. Crystallization parameters for PA12 and PA12/SEBS-*g*-MA blends during non-isothermal cooling process.

	R (°C min^{-1})	T_0 (°C)	T_p (°C)	ΔT_c (°C)	X_c (%)
N12	10	154.5	151.9	29.00	34.0
	20	150.6	146.3	36.62	
	30	150.0	143.0	39.50	
NS10	10	154.8	151.6	27.70	36.7
	20	151.3	147.0	33.87	
	30	150.0	144.1	40.42	
NS20	10	154.9	152.1	27.90	37.8
	20	150.9	147.5	31.98	
	30	151.0	144.5	40.50	
NS35	10	154.8	151.9	28.10	39.7
	20	151.2	147.0	33.51	
	30	151.0	143.7	38.34	
NS50	10	154.0	151.5	27.30	54.4
	20	151.2	146.7	34.78	
	30	150.5	144.0	36.50	

cooling rate slows down the mobility of polymeric chains at a higher undercooling and reduces the time allowed for its crystallization, which leads to lower crystallization temperature. At any cooling rate there is almost no change in T_0 and T_p with the incorporation of an increase in SEBS-*g*-MA content into PA12 matrix. The ΔT_c values decrease as Φ_d enhances from 10 to 50 wt% at any cooling rate. As explained in the previous work, SEBS-*g*-MA slightly acts as a nucleating agent by providing a surface for crystallization to PA12 matrix and thus increases the crystallinity percentage. The increased nucleation sites in the system should lead to an increase in the crystallization temperature, but the adhesion between polar moiety of PA12 and MA group of SEBS-*g*-MA impart restriction to the mobility of polymer chains, which decreases the crystallization temperature. Overall, the two contradicting effects are responsible for no change in T_p and T_0. The degree of undercooling, ΔT_c, considered as the driving force to the crystallization process, increases with increase in cooling rate in PA12 and the blends. However at corresponding cooling rates the parameter in the blends decreases from PA12 which may be due to the phase adhesion.

From the DSC cooling scans, the value of relative crystallinity (X_t) at different cooling rates can be calculated using the following equation[9–11]

$$X_t = \frac{\int_{T_0}^{T} (\mathrm{d}H_c/\mathrm{d}T)\,\mathrm{d}T}{\int_{T_0}^{T_\infty} (\mathrm{d}H_c/\mathrm{d}T)\,\mathrm{d}T} = \frac{A_0}{A_\infty}, \quad (1)$$

where T_0 is the initial temperature at which crystallization starts, T the temperature at the time t, T_∞ the temperature at which the crystallization process is completed, and A_0 and A_∞ are the areas under the DSC scans from T_0 to T and T_0 to T_∞, respectively. The variations of X_t as a function of temperature T for PA12 and PA12/SEBS-*g*-MA blends are shown in figure 2. All the samples show reverse sigmoidal shape curves indicating the lag effect of cooling rate in the crystallization process.[12]

Figure 3 shows the plot of X_t *vs.* time (t), where temperature axis from figure 3 was converted into time scale by using[13]

$$t = \frac{T_0 - T}{R}, \quad (2)$$

where T is the temperature at crystallization time t, T_0 the initial (onset, i.e., at $t = 0$) temperature of crystallization and R the cooling rate. All the curves were S-shaped indicating a decrease in time for complete crystallization with increasing cooling rates for PA12 and PA12/SEBS-*g*-MA blends, as quick cooling provides less time for polymer to crystallize.[14] Also, the experimental half-time of crystallization, $t_{1/2(exp)}$, determined at $X_t = 0.5$ (figure 3), reduces with increasing cooling rates. The value of $t_{1/2(exp)}$ is found to be slightly lower in case of NS10, NS20 and NS35 as compared to N12 for corresponding cooling rates signifying the nucleating effect of SEBS-*g*-MA copolymer (table 4). This reflected the alteration in the rate of growth of the PA12 crystals during crystallization.

The kinetics of the crystallization process is analysed by the well-known classical Avrami equation.[15–17] Although the Avrami model was given for isothermal crystallization but it also provides information of nucleation and crystal growth during non-isothermal crystallization of polymers.[18–21]

The isothermal crystallization kinetics is controlled by random nucleation and growth of the crystals. The relative crystallinity (X_t) at any time t is given by

$$X(t) = 1 - \exp[-k(T)(t - t_0)^n], \quad (3)$$

where n is the Avrami exponent, which gives information about the type of nucleation and crystal growth dimension, k the Avrami rate constant which includes both nucleation and growth rate parameter (min^{-n}). The simplified double logarithmic expression of equation (3) can be written as

$$\ln[-\ln(1 - X_t)] = \ln k + n \ln t. \quad (4)$$

The slope and the intercept of the best fitted line from the plot of $\ln[-\ln(1 - X_t)]$ *vs.* $\ln t$ for each cooling rate gives the value of the Avrami parameters n and k. These parameters are then used to predict the crystalline morphology and the type of crystal growth for particular crystallization conditions. However, these parameters show different significance in case of non-isothermal crystallization compared to isothermal crystallization because under non-isothermal conditions temperature changes with time affects both nuclei formation and growth rate of the crystallites.

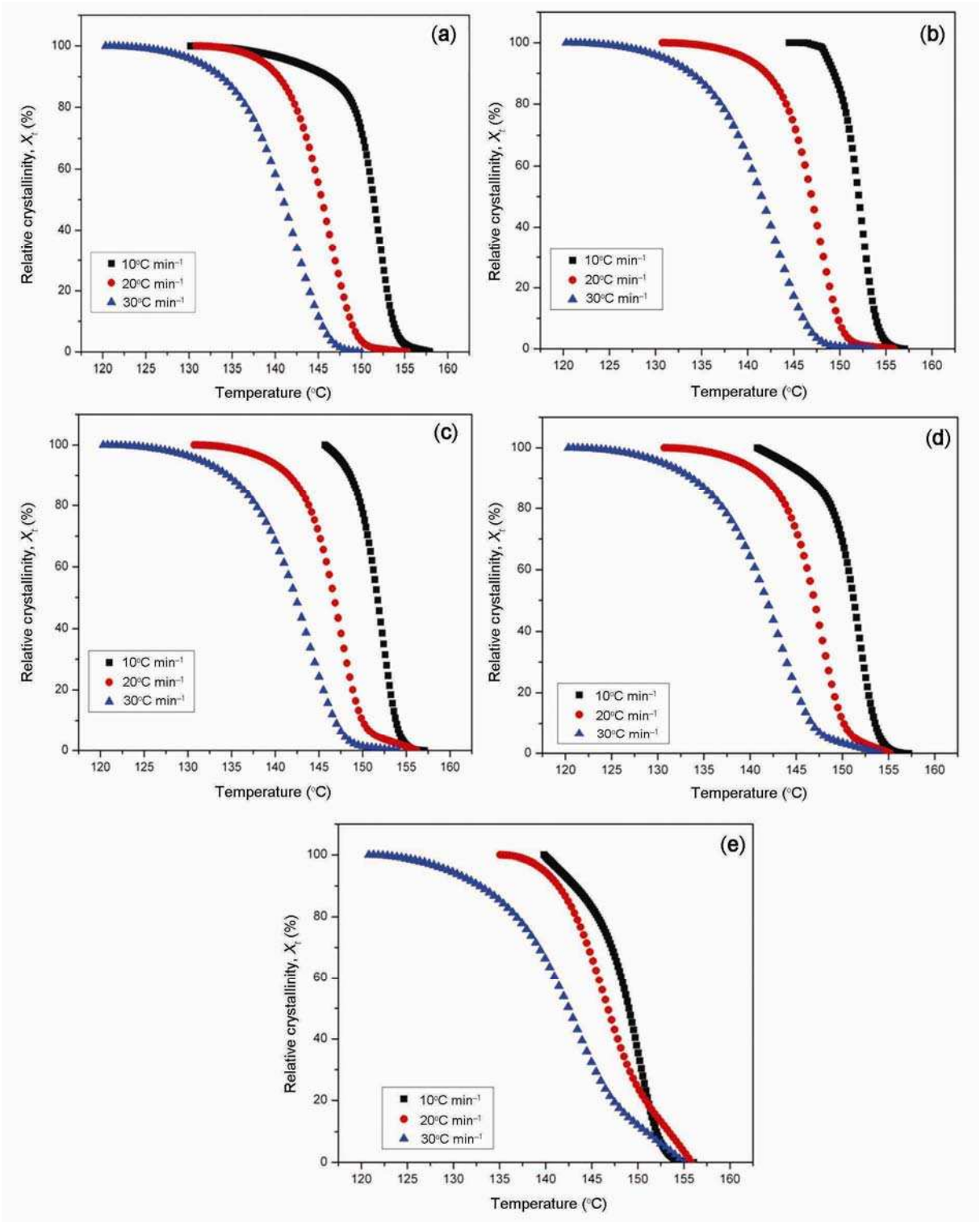

Figure 2. Variation of relative crystallinity *vs.* temperature at various cooling rates during non-isothermal crystallization for (**a**) N12, (**b**) NS10, (**c**) NS20, (**d**) NS35 and (**e**) NS50.

The time to reach 50% of relative crystallinity, $t_{1/2}$, is calculated by using

$$t_{1/2} = [\ln 2/k]^{1/n}. \quad (5)$$

The natures of the curves represent different regimes of the crystallization process. The starting region, $X_t < 0.05$, is called as induction period where primary nuclei are formed. This region can be neglected for the calculation

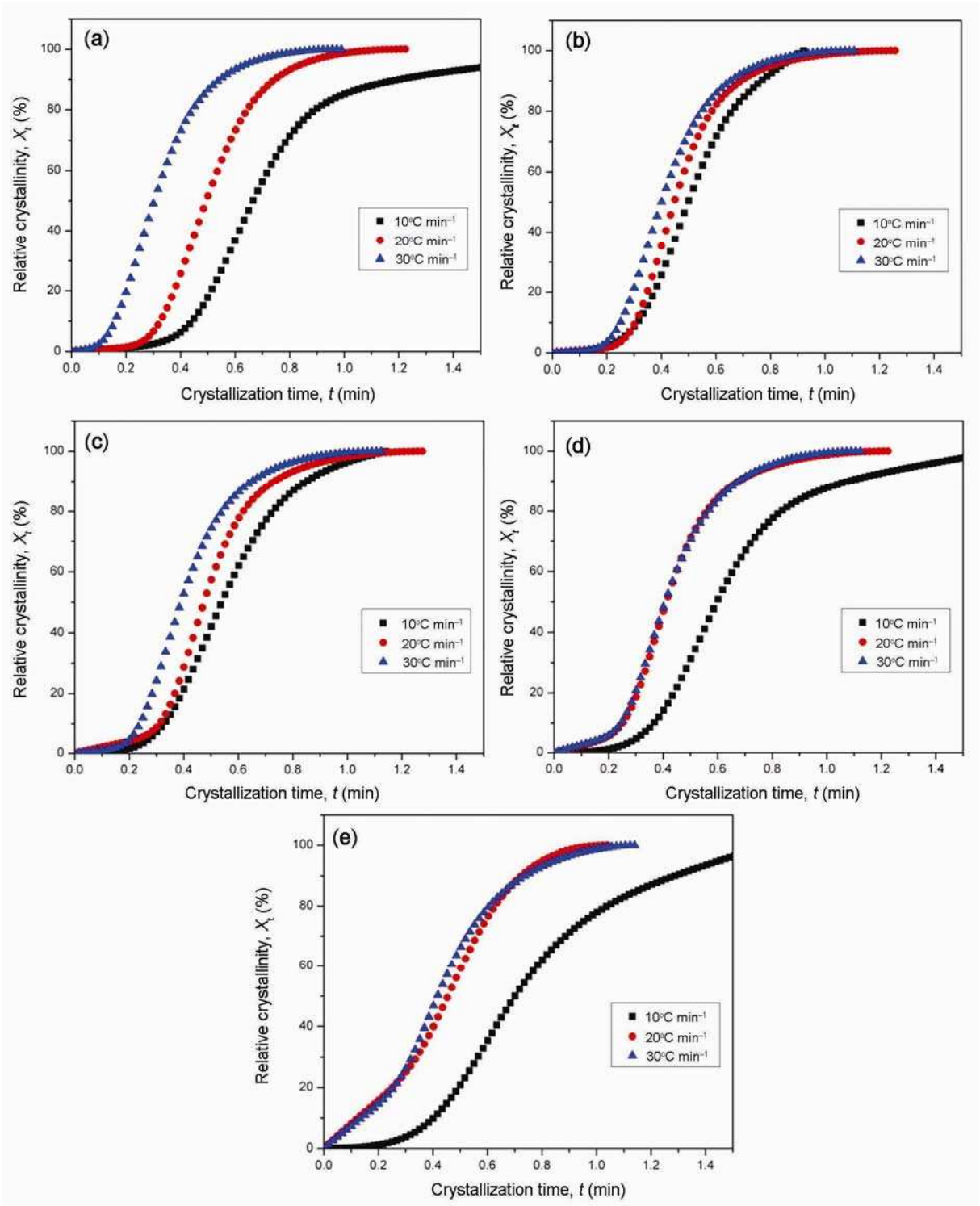

Figure 3. Variation of relative crystallinity *vs.* time at various cooling rates during non-isothermal crystallization for (**a**) N12, (**b**) NS10, (**c**) NS20, (**d**) NS35 and (**e**) NS50.

of crystallization parameters as the values are too low. The intermediate region, $0.05 < X_t < 0.80$, can be termed as primary crystallization region where faster growth of actual PA12 crystallites occur. Here the straight line variations were fitted to calculate the Avrami parameters with good regression coefficient ($r^2 > 0.98$). The end region, called secondary crystallization, $0.80 < X_t < 0.99$, is a period of slow crystallization where nylon molecules grow on already formed crystallites (impingement) and increase the thickness of the crystallites which enhances

Table 4. Avrami analysis for non-isothermal crystallization behaviour of PA12 and PA12/SEBS-*g*-MA blends.

		Non-isothermal kinetics										
		Primary crystallization $5 < X_t < 80$			Secondary crystallization $80 < X_t < 99$			Overall crystallization $5 < X_t < 99$				
Designation	R (°C min^{-1})	n	k (min^{-n})	r^2	n	k (min^{-n})	r^2	n	k (min^{-n})	r^2	$t_{1/2}$ (s) (calculated)	$t_{1/2}$ (s) (experimental)
N12	10	4.0	3.15	0.986	1.3	1.85	0.930	2.0	1.22	0.880	45	40
	20	4.0	11.47	0.990	2.1	4.30	0.999	3.1	5.30	0.972	31	30
	30	2.7	16.44	0.994	1.6	6.42	0.999	2.2	8.60	0.982	19	17
NS10	10	4.4	4.95	0.997	2.6	4.48	0.990	3.4	6.04	0.989	31	30
	20	3.6	12.18	0.991	1.8	4.05	0.998	2.4	4.95	0.965	26	27
	30	3.6	16.44	0.987	2.0	4.95	0.998	2.7	6.60	0.969	26	24
NS20	10	3.5	5.47	0.993	2.4	3.40	0.989	3.0	3.81	0.986	34	32
	20	4.0	12.18	0.994	1.8	4.01	0.998	3.0	5.05	0.963	31	28
	30	3.4	14.80	0.986	1.8	5.05	0.999	2.6	6.00	0.968	26	24
NS35	10	3.4	3.50	0.988	1.5	2.05	0.981	2.3	1.84	0.946	39	36
	20	3.5	13.40	0.995	1.7	4.05	0.997	2.5	5.47	0.966	26	25
	30	3.4	12.18	0.993	1.9	4.85	0.998	2.6	6.17	0.977	26	24
NS50	10	2.9	2.18	0.986	2.2	1.41	0.981	2.5	1.36	0.978	45	42
	20	2.2	4.17	0.989	2.7	5.50	0.996	2.4	5.00	0.994	26	27
	30	2.2	4.48	0.991	2.0	4.20	0.994	2.1	4.39	0.996	25	25

the crystallinity to some extent. The Avrami parameters such as n, k and $t_{1/2}$ (calculated) of primary, secondary and overall crystallization for PA12 and PA12/SEBS-*g*-MA blends are summarized in table 4.

The Avrami exponent n is composed of two terms, represents dimension of the growing crystals (integer numbers 1, 2 or 3, corresponding to one-, two- or three-dimensional crystal) and nucleation kinetics (zero for instantaneous or heterogeneous nucleation, 1 for sporadic or homogeneous nucleation, 0–1 for decreasing nucleation and >1 for increasing nucleation).[22] The values of the Avrami exponent n in the primary crystallization region fall in the range of 2.7–4.0 for N12, 3.6–4.4 for NS10, 3.4–4.0 for NS20, 3.4–3.5 for NS35 and 2.2–2.9 for NS50 (table 4). It can be seen that n-value lies between 3 and 4 for N12 and its blend with SEBS-*g*-MA up to 35 wt% of SEBS-*g*-MA but decreases to 2–3 with 50 wt% of SEBS-*g*-MA.

The Avrami exponent n in the range of 3–4 indicates spherulitic crystal growth with random/heterogeneous nucleation whereas in the range of 2.2–2.9, it implies mixture of two-dimensional, three-dimensional and circular disc-like crystal growth. It reflects the presence of different nucleating/crystallization kinetics of the samples due to their different structure. In NS50, although SEBS-*g*-MA acts as a nucleating agent, the confinement of the PA12 chain mobility due to the availability of increased number of MA groups dominated the crystallization kinetics which in turn reduces the value of n. These n-values are quite low compared to other PA systems, where the parameter was $\gg 4$.[21,23,24] In those cases the crystal morophology was suggested to a continuous change from needle-like to disc-like or spherulite shapes. Spherulite impingement or growth of spherulite in between already formed spherulites also enhanced the value on n beyond 4. In the present system, the n-value varied between 2 and 4 describing the existence of disc-like to spherulitic structures.[25] This may be due to lesser amide/hydrocarbon ratio in PA12, which restricted the formation and growth of crystal morphology even in non-isothermal crystallization.

The value of rate of crystallization is highest at the fastest cooling rate of 30°C min^{-1} as was also reported in PA6/SEBS-*g*-MA blends.[26] The crystallization rates at all the cooling rates were marginally higher up to NS35, although the value at 30°C min^{-1} cooling rate decreased in NS20 and NS35. The enhancement of k-value may be due to the surface provided for crystal initiation by the dispersed phase. Some extent of phase adhesion is also possible, however as the amide groups are far apart in N12, this phase adhesion may be random, which could not decrease the rate of crystallization and hence could not prevent the PA12's crystal formation. The decrease in k-value at 30°C min^{-1} cooling rate may be due to an impingement and crowding effect. It may be noted that the k-value is much lower in NS50, suggesting the dependence of the growth rate on the separation of the phases. It may be considered that at 50% SEBS-*g*-MA polymer content the phase interaction may be the highest. Although the dispersed phase may still provide surface for crystal initiation, the large volume of the former with its co-continuous morphology with N12 may cause impingement and crowding of the crystal nuclei, which

may not find space for further growth that ultimately lowers the value of k.

In the secondary crystallization region, where $0.80 < X_t < 0.99$, relatively lower value of k are obtained due to the fact that crystallization of nylon molecule take place over the already formed crystals, i.e., impingement of already formed crystals occurs. The observed value of n is in the range of 1.3–2.7, suggesting that all forms of structures grow from small dimensions at much decreased nucleation rate. The value of k is in the range of 1.41–6.42. Both the value of n and rate constant k is much lower in this region as compared to that of primary crystallization, because crystals grow on already grown crystallites at reduced nucleation and growth rates, the latter due to impingement and crowding effects.

The Avrami equation is applied to overall non-isothermal crystallization kinetics by the plot of $\ln[-\ln(1 - X_t)]$ against $\ln(t)$ for X_t = 5–99%, figure 4. The overall n-values

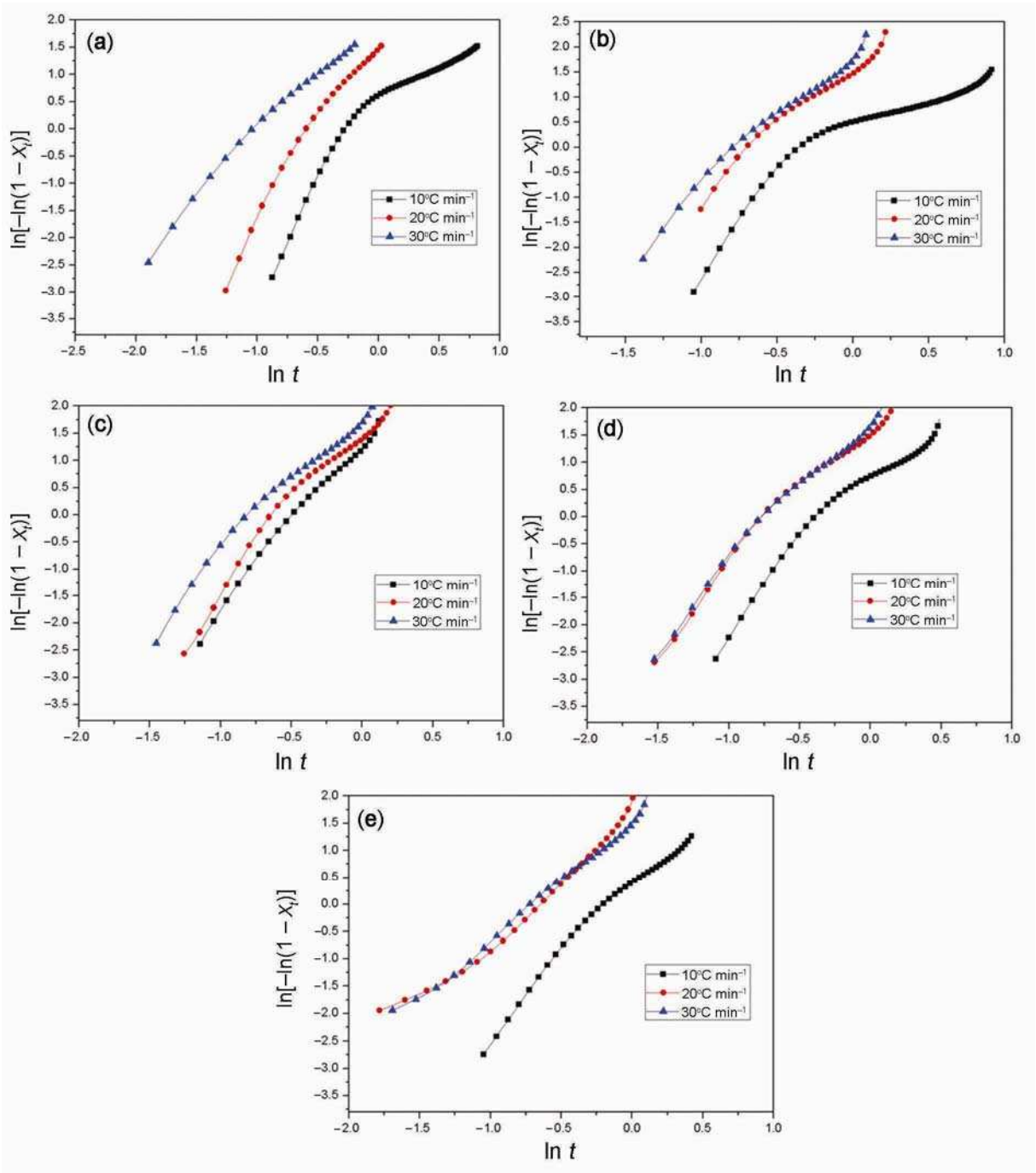

Figure 4. Avrami plots of $\ln[-\ln(1 - X_t)]$ *vs.* $\ln t$ during non-isothermal crystallization for (**a**) N12, (**b**) NS10, (**c**) NS20, (**d**) NS35 and (**e**) NS50.

predicted from linear fit to the curve varies from 2.0 to 3.4 with regression coefficient ($r^2 > 0.88$), suggesting the dominance of disc-like and spherulitic crystal growth. It can be seen that $t_{1/2}$ values for the blends decreased with the increase in cooling rate, indicating that higher the cooling rate lower the time for complete crystallization. In addition, for a given cooling rate $t_{1/2}$ values for PA12/SEBS-*g*-MA blends up to 35 wt% of SEBS-*g*-MA, are slightly lower than that of neat PA12 which suggests that the incorporation of SEBS-*g*-MA increases the crystallization rate of PA12. The $t_{1/2}$ value for NS50 is comparable or slightly higher at higher cooling rate than that of PA12. This is an outcome of decreased growth rate of transformation (k), as a result of limited space for nucleation or rejection of SEBS-*g*-MA domain and growth becomes simple. The complexity in the non-isothermal crystallization arises with the increase in cooling rate, which can be attributed to the heterogeneity in the system as time given for crystallization decreases which could not bring complete crystallization of the system. Also, the Avrami equation which actually proposed for isothermal crystallization kinetics when applied to non-isothermal kinetics gives complexity in the nucleation mechanism.

3.3 *Jeziorny correction for the rate constant*

In non-isothermal crystallization process, temperature changes with time which affects the rate of both nuclei formation and spherulitic growth as both the parameters are temperature dependent. Considering the effect of cooling rate, the kinetic parameter k of the Avrami equation under non-isothermal crystallization was modified by Jeziorny.[27]

$$\ln(k') = \ln(k)/R, \tag{6}$$

where k is the crystallization rate constant and k' the modified crystallization rate constant with respect to cooling rate R. The half-time of crystallization, $t_{1/2}$, for the non-isothermal crystallization can be calculated after correcting the crystallization constant k'

$$t_{1/2} = \left[\frac{\ln 2}{k'}\right]^{1/n}. \tag{7}$$

Table 5 shows the Jeziorny parameters after eliminating the effect of cooling rate. The values of crystallization rate k' for pure PA12 and PA12/SEBS-*g*-MA blends exhibit marginal variation in primary and overall crystallization range. The crystallization half-time, $t_{1/2}$, for pure PA12 and PA12/SEBS-*g*-MA blends remain constant within 2–3 s variation. This also suggests that $t_{1/2}$ is also a measure of crystallization rate, i.e., lower values denote higher crystallization rate.

3.4 *Isothermal kinetics using the Avrami equation*

Isothermal DSC runs were conducted at 148°C for pure PA12 and PA12/SEBS-*g*-MA blends in order to compare the change in crystallization behaviour under the isothermal conditions (figure 5a–c). The DSC exotherms and the corresponding variation of relative crystallinity X_t with time t during isothermal run for pure PA12 and PA12/SEBS-*g*-MA blends are presented in figure 5a and b, respectively. Avrami plots of $\ln[-\ln(1 - X_t)]$ against

Table 5. Jeziorny parameters evaluated for non-isothermal crystallization kinetics of PA12 and PA12/SEBS-*g*-MA blends.

	Primary crystallization		Overall crystallization	
Designation	R (°C min^{-1})	K' (min^{-n})	K' (min^{-n})	$t_{1/2}$ (s)
N12	10	1.12	1.02	49
	20	1.13	1.09	52
	30	1.10	1.07	49
NS10	10	1.17	1.20	51
	20	1.13	1.08	50
	30	1.10	1.06	51
NS20	10	1.19	1.14	51
	20	1.13	1.08	52
	30	1.09	1.06	51
NS35	10	1.13	1.06	50
	20	1.14	1.09	50
	30	1.09	1.06	51
NS50	10	1.08	1.03	51
	20	1.07	1.08	50
	30	1.05	1.05	49

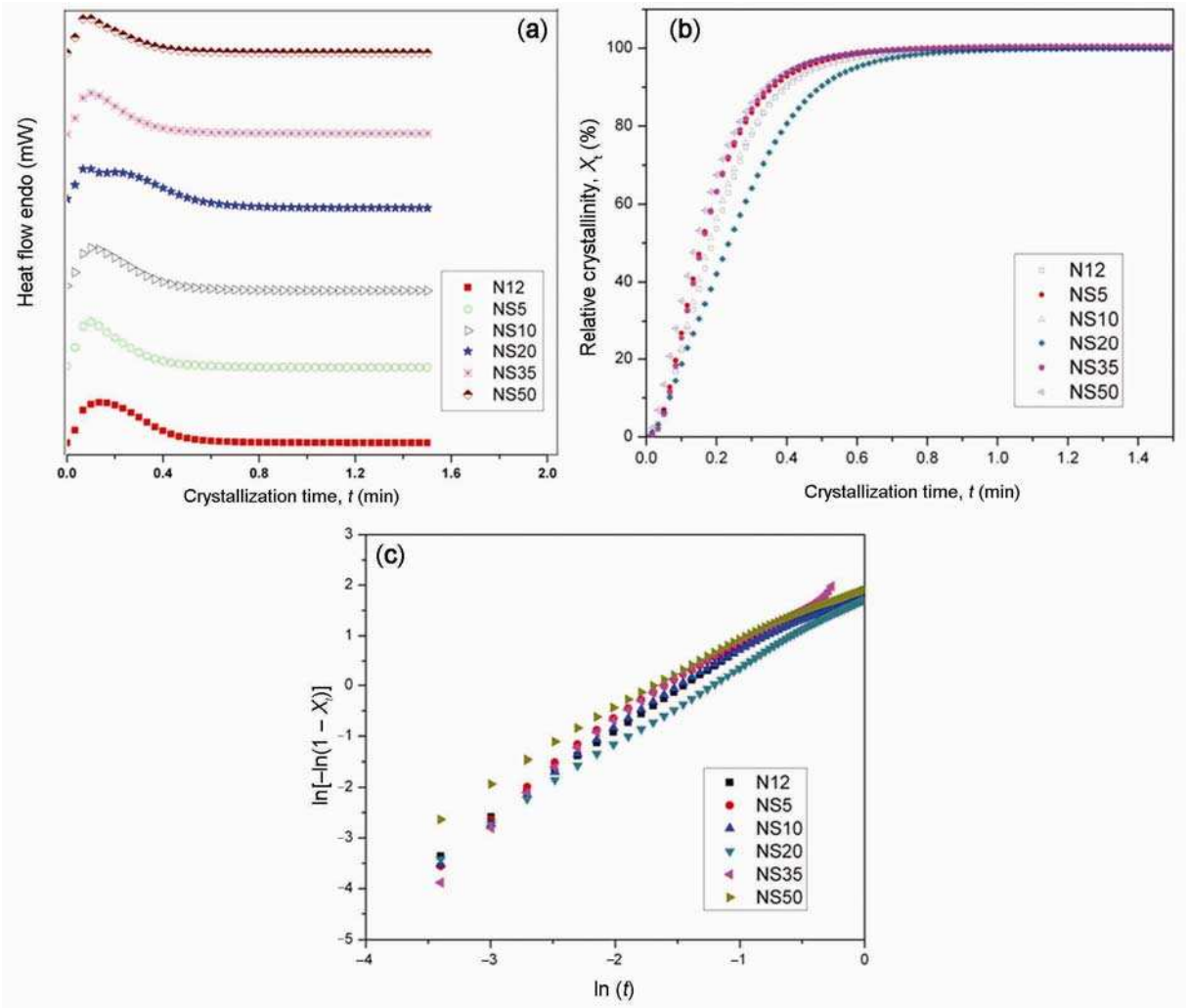

Figure 5. Isothermal crystallization parameter variations for PA12/SEBS-*g*-MA blends at various blend compositions: (**a**) isothermal crystallization exotherms, (**b**) relative crystallinity *vs.* crystallization time and (**c**) Avrami plots of $\ln[-\ln(1 - X_t)]$ *vs.* $\ln t$.

ln(*t*), figure 5c, are linear with regression coefficient values (≈ 0.99), suggesting the validity of the Avrami equation for isothermal crystallization. The nucleation and growth mechanism are quite similar in the pure components and the blends, table 6. The crystallization rate constant *k* is in the range of 5.9–9.9 min^{-n}. The overall rate of crystallization can be characterized by half-time of crystallization ($t_{1/2}$) and the value of $t_{1/2}$ vary from 10 to 14 s for pure PA12 and PA12/SEBS-*g*-MA blends.

The range of *n*-value between 1.1 and 1.5 implies shapes of crystal growing from small dimension with a mixture of one-dimensional, needle-like to two-dimensional growth mechanism under random and instantaneous nucleation with diffusion-controlled growth of thermal and athermal nucleation mechanisms.[2] The value of *k* are in the same range observed in non-isothermal crystallization process, table 6. The decrease in *k* is an indicative of slower rate of isothermal crystallization.

The trend of rate constant does not follow a definite pattern with the increase in concentration of SEBS-*g*-MA. Relatively higher value of *k*, i.e., 7.3 min^{-n} was found in N12 and NS5 possibly because of homogeneous nucleation in nylon-rich phase. The lower value of *k* for NS10 and NS20 could be due to the dominating effect of phase adhesion which restricts the polymer mobility and thus decreses the growth of crystal formation. The higher value of *k* for NS35 could be due to the effect of coalescence of SEBS-*g*-MA domains giving nylon-12-rich region and hence diffusion is much easier giving rise to faster growth of crystals.[21]

3.5 *Nucleation activity*

A method proposed by Dubreva and Gutzowa[28] was used to evaluate the nucleation ability of the SEBS-*g*-MA in PA12/SEBS-*g*-MA blends. In case of homogeneous

Table 6. Avrami analysis for isothermal crystallization behaviour of PA12 and PA12/SEBS-*g*-MA blends.

	Isothermal kinetics				
Designation	n	k (min^{-n})	$t_{1/2}$ (s) (calculated)	$t_{1/2}$ (s) (experimental)	r^2
N12	1.5	7.38	12	12	0.988
NS5	1.4	7.30	11	10	0.970
NS10	1.4	6.60	12	10	0.980
NS20	1.5	5.90	14	14	0.997
NS35	1.5	9.97	10	11	0.992
NS50	1.1	7.17	8	8	0.988

nucleation from the melt of PA12, the cooling rate R can be written as

$$\log(R) = A - \frac{B}{2.303\Delta T_p^2}, \tag{8}$$

where ΔT_p is defined as $T_m - T_p$, while T_m and T_p are the peak temperatures of melting and crystallization, respectively and A and B the constants. In the melt state of the blends for hetrogeneous nucleation in the presence of a nucleating agent or any other surface providing material, the cooling rate is written as

$$\log(R) = A - \frac{B^*}{2.303\Delta T_p^2}, \tag{9}$$

where B^* is a constant. Thus, the nucleation activity, Φ, is defined by the ratio of B^*/B. The value of $\Phi = 0$ is an indication that the substrate is an active nucleating substrate and $\Phi = 1$ stands for inert or non-nucleating particles. The constants B and B^* can be derived from the slope of the linear plot of $\log R$ *vs.* $1/\Delta T_p^2$ for the pure polymer and the blends, figure 6. The values of B, B^* and Φ are presented in table 7. It can be noted that Φ is slightly less than 1 for blend compositions, indicating an extent of the nucleating effect of SEBS-*g*-MA copolymer. Although interfacial reaction between SEBS-*g*-MA and PA12 would have provided nucleation sites for crystallization of PA12, the adhesion is limited to some extent because of the limited amount of MA in SEBS-*g*-MA copolymer (1.4–2.0%). Also the homogeneous crystallization of nylon-rich phase due to hydrogen bonding is present in the PA12/SEBS-*g*-MA blends. Thus, a mixture of nucleation as well as confinement of PA12 molecules or impingement of spherulites are the deciding factors for crystallization kinetics as stated earlier.

3.6 *Activation energy of non-isothermal crystallization*

The activation energy of crystallization, ΔE, for PA12 and blend compositions was determined by employing Kissinger (equation 10), Takhor (equation 11) and

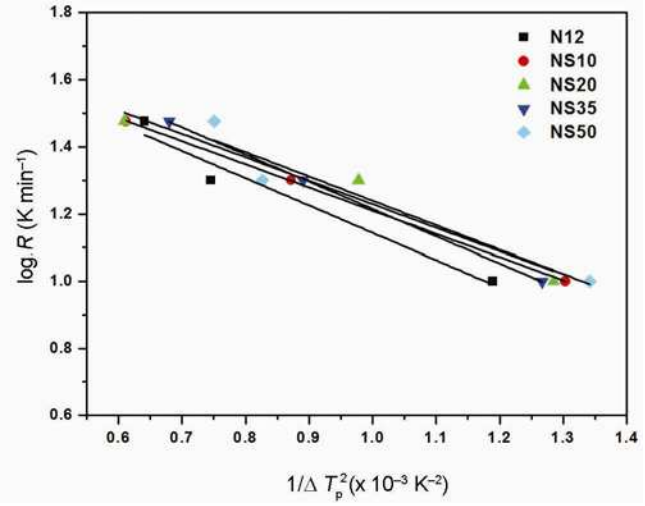

Figure 6. Plots for nucleation activity of pure PA12 and PA12/SEBS-*g*-MA blends by the Dobreva and Gutzowa method.

Table 7. Nucleation activity for various PA12/SEBS-*g*-MA blends at different blend compositions.

Sample	Slope (B or B^*)	Nucleation activity (Φ)
N12	813	1.00
NS10	691	0.84
NS20	699	0.85
NS35	812	0.99
NS50	726	0.89

Augis and Bennett (equation 12) methods.[21,29–31] All these methods have used the relationship between peak temperature T_p of non-crystallization exotherms and cooling rate R to obtain the activation energy:

Kissinger method:

$$\left[\frac{d\left[\ln(R/T_p^2)\right]}{d(1/T_p)}\right] = -\frac{\Delta E}{R_g}. \tag{10}$$

Takhor method:

$$\left[\frac{d[\ln R]}{d(1/T_p)}\right] = -\frac{\Delta E}{R_g}. \tag{11}$$

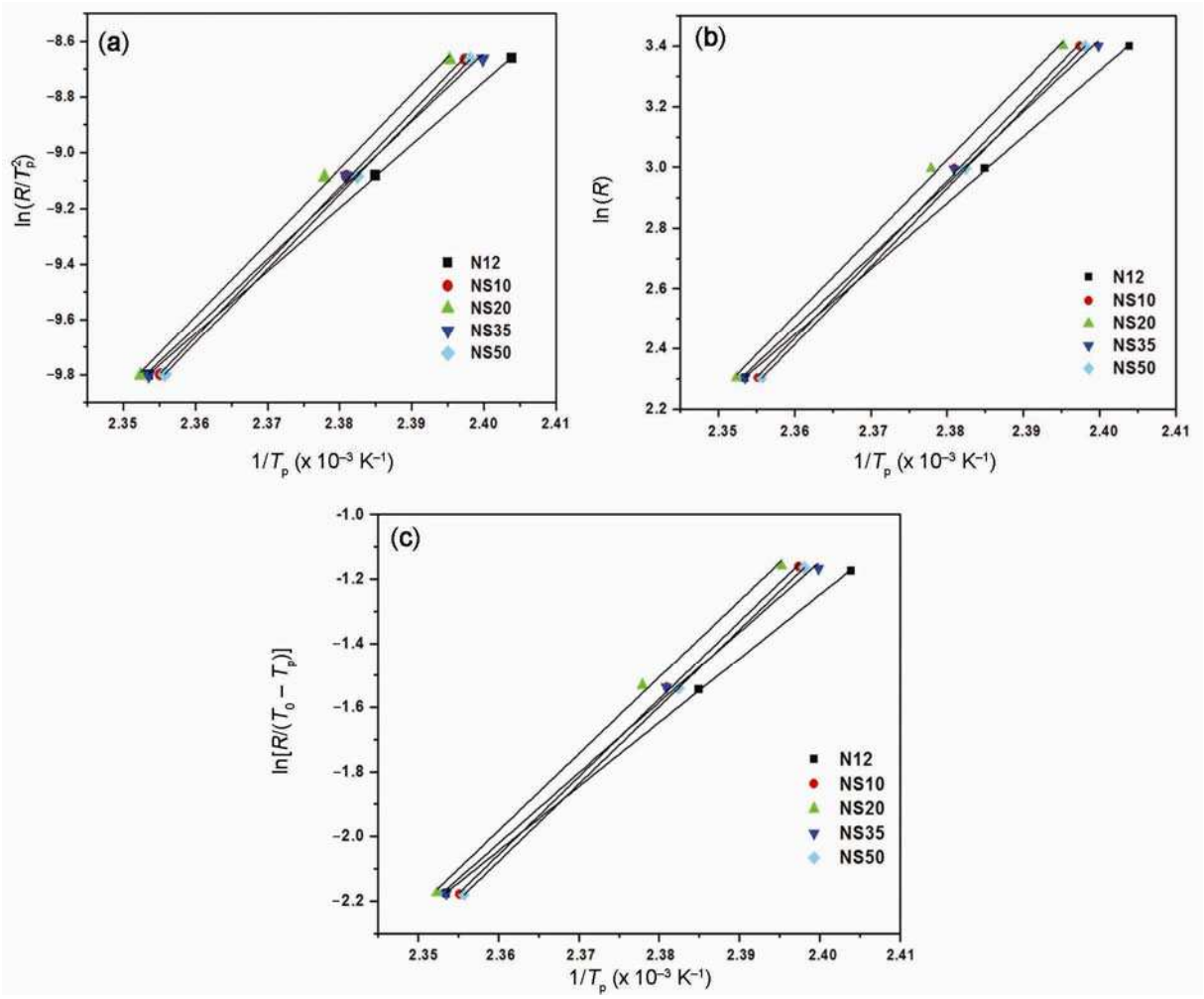

Figure 7. Activation energy of crystallization: (**a**) Kissinger method, (**b**) Takhor method and (**c**) Augis-Bennett method.

Augis-Bennett method:

$$\left[\frac{\mathrm{d}\left[\ln(R/(T_0 - T_\mathrm{p}))\right]}{\mathrm{d}(1/T_\mathrm{p})}\right] = -\frac{\Delta E}{R_\mathrm{g}}, \qquad (12)$$

where T_0 is the initial reference temperature from the melt state (assumed as 240°C), T_p the crystallization peak temperature, R_g the universal gas constant (R_g = 8.3145 J mol^{-1} K^{-1}), and R the cooling rate. The values of activation energy estimated from the slopes of the straight lines fitted to the plots based on equations (10)–(12), figure 7a–c, are listed in table 8. Although the absolute value of ΔE is found to be different for different methods of evaluation, all the methods show an increase in ΔE with the incorporation of SEBS-*g*-MA for all the blend compositions studied. In general, activation energy represents the barrier for crystallization in two-phase immiscible blends. It depends on several factors such as difference in the thermal conductivity of the amorphous and crystallizable components, kinetic energy dissipated for rejection, melt viscosity of the system, energy required during engulfing and deformation of the non-crystallizable phase, energy needed to overcome the inertia of crystallizable phase and for interface formation.[32,33] However, the SEBS-*g*-MA has facilitated the crystallization of PA12 by providing surface for crystallization but all these complexities showed that much more energy is needed for crystallization of PA12 molecule from the primary nuclei. This increases the ΔE for

Table 8. Activation energy values for PA12/SEBS-*g*-MA blends at different blend compositions.

	Activation energy (E) (kJ mol^{-1})		
Sample	Kissinger	Takhor	Augis-Bennett
N12	189.42	182.42	166.51
NS10	216.76	209.77	193.81
NS20	221.52	221.52	198.40
NS35	201.71	201.70	178.75
NS50	215.76	215.76	192.83

PA12/SEBS-*g*-MA blends compared to that of PA12 matrix.

4. Conclusion

The non-isothermal crystallization and isothermal crystallization kinetics of PA12 and PA12/SEBS-*g*-MA blends were studied by using the Avrami model. Results showed that the crystallization kinetics under non-isothermal condition is more complicated as compared to that under isothermal conditions. The rate of transformation during isothermal kinetics increases with the increase in cooling rate. The Zeziorny method was successfully used to predict the crystallization growth after taking into account the cooling rate. The value of Avrami exponent n was found to be in the range of 3–4 for pure PA12 and PA12/SEBS-*g*-MA blends up to 35 wt% of SEBS-*g*-MA, indicating spherulitic crystal growth with random/heterogeneous nucleation whereas the addition of 50 wt% of SEBS-*g*-MA (n = 2–3) gives mixture of two-dimensional, three-dimensional and circular disc-like crystal growth. The morphology of the dispersed phase greatly affected the crystal growth during primary crystallization. The value of crystallization growth constant k was observed to be very low in case of NS50 due to the limited space for growing crystals.

The value of n during isothermal crystallization kinetics is very low and lies between 1.1 and 1.5, indicating the crystal growth from small dimension with a mixure of one-dimensional, needle-like, to two-dimensional growth mechanism with diffusion controlled growth of thermal and athermal nucleation mechanisms.

An extent of nucleating ability of SEBS-*g*-MA was revealed in the nucleation activity analysis. At lower concentration of SEBS-*g*-MA (upto 35 wt%), faster crystallization was shown by reduced $t_{1/2}$ due to the nucleating activity of SEBS-*g*-MA. Whereas at higher SEBS-*g*-MA concentration the dominance of morphological changes over nucleating ability has delayed the crystallization process and thus increased the $t_{1/2}$ during non-isothermal crystallization. The activation energy values were higher for PA12/SEBS-*g*-MA blends because of the phase adhesion which restricted the chain mobility so that the blends required more energy for crystallization. It can be concluded that the morphology changes by incorporating 20 wt% of SEBS-*g*-MA in PA12 (showed in SEM images) and faster crystallization at this stage is responsible for balance of overall properties in NS20 blend. This study was further used to express mechanical properties of blends in our already published work.

References

1. Marco C, Ellis G, Gómez M A and Arribas J M 2003 *J. Appl. Polym. Sci.* **88** 2261
2. Asadinezhad A *et al* 2007 *J. Appl. Polym. Sci.* **106** 1964
3. Meng H, Sui G X, Xie G Y and Yang R 2009 *Compos. Sci. Technol.* **69** 606
4. Jain S, Goossens H, van Duin M and Lemstra P 2005 *Polymer* **46** 8805
5. Pathmanathan K and Johari G P 1993 *J. Polym. Sci. Part B: Polym. Phys.* **31** 265
6. Ulf H and Rohde-Liebenau W 1999 In *Polymer data handbook* (ed) J E Mark (Oxford University Press) p 225
7. Kohan M I 1995 *Nylon plastics handbook* (Hanser)
8. Jose S, Thomas P S, Thomas S and Karger-Kocsis J 2006 *Polymer* **47** 6328
9. Hay J N and Sabir M 1969 *Polymer* **10** 203
10. Hay J N, Fitzgerald P A and Wiles M 1976 *Polymer* **17** 1015
11. Hay J N 1979 *Br. Polym. J.* **11** 137
12. Zhang F, Zhuo L, Xiong Y and Xu W 2008 *J. Polym. Sci. Part B: Polym. Phys.* **46** 2201
13. Kim S H, Ahn S H and Hirai T 2003 *Polymer* **44** 5625
14. Liu M *et al* 2003 *Polymer* **44** 2537
15. Avrami M J 1939 *J. Chem. Phys.* **7** 1103
16. Avrami M J 1940 *J. Chem. Phys.* **8** 212
17. Avrami M J 1941 *J. Chem. Phys.* **9** 177
18. Supaphol P, Dangseeyun N, Srimoaon P and Nithitanakul M 2003 *Thermochim. Acta* **406** 207
19. Apiwanthanakorn N, Supaphol P and Nithitanakul M 2007 *Polym. Test.* **23** 817
20. Supaphol P 2001 *J. Appl. Polym. Sci.* **78** 388
21. Balamurugan G P and Maiti S N 2008 *J. Appl. Polym. Sci.* **107** 2414
22. Sperling L H 1992 *Handbook of introduction to physical polymer science* (John Wiley & Sons) 2nd ed., p 234
23. Weng W, Chen G and Wu D 2003 *Polymer* **44** 8119
24. Liu T, Mo Z, Wang S and Zhang H 1997 *Polym. Eng. Sci.* **37** 568
25. Rinawa K, Maiti S N, Sonnier R and Cuesta J-M L 2014 *Polym. Bull.* **71** 1131
26. Hemlata and Maiti S N 2012 *J. Polym. Res.* **19** 9926
27. Jeziorny A 1978 *Polymer* **19** 1142
28. Dobreva A and Gutzow I 1993 *J. Non-Cryst. Solids* **162** 1
29. Augis J A and Bennett J E 1978 *J. Therm. Anal.* **13** 283
30. Kissinger H E 1956 *J. Res. Natl. Bur. Stand.* **57** 217
31. Takhor R L 1971 *Advances in nucleation and crystallization of glasses* (Columbus: American Ceramics Society) p 166